Charm and Bottom Production at RHIC and LHC

R. Vogt

Nuclear Science Division, Lawrence Berkeley National Laboratory, Berkeley, CA 94720, USA

Physics Department, University of California, Davis, CA 95616, USA

Outline

- **Charm and Bottom Production**
- **Transverse Momentum Distributions**
- **Electrons from Heavy Flavor Decays**

Another Birthday, 20 Years Ago...

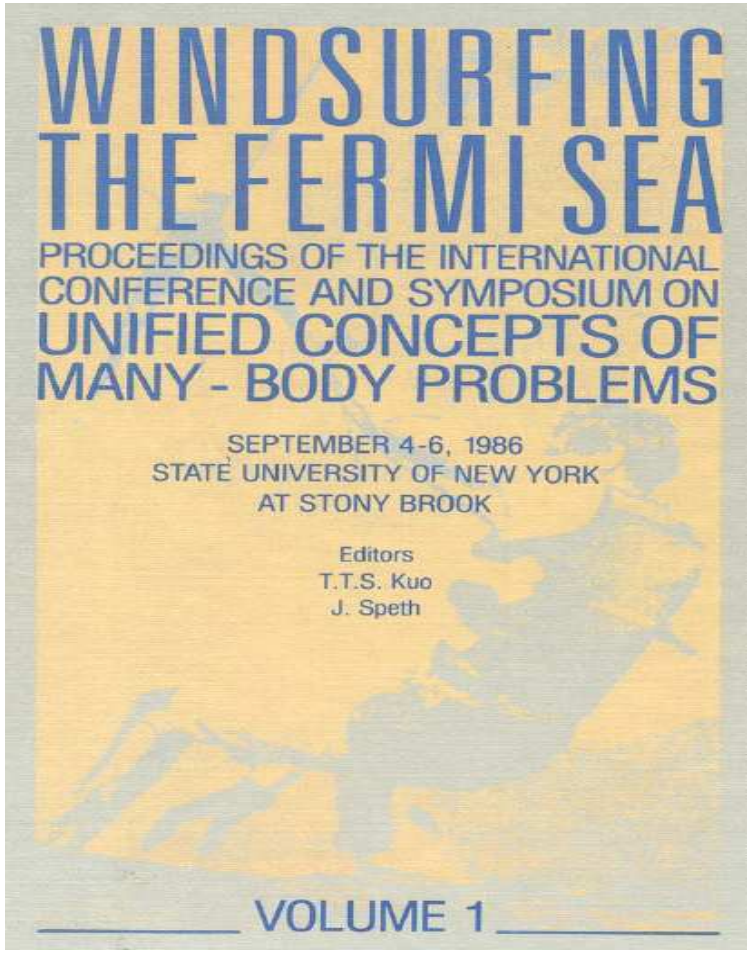

Herding Cats?

CERN, Geneva 1994
LBL, Berkeley 1994
ECT*, Trento 1995
INT, Seattle 1996
CFIF, Lisbon 1997
INT, Seattle 1998
JYFL, Jyväskylä 1999
BNL, New York 2000
NBI, Copenhagen 2001

Charm as a Probe of Heavy Ion Collisions

Hard probe produced in the initial nucleon-nucleon collisions

Interacts strongly so its momentum can be modified by collisions during the evolution of the system leading to effects such as

- **Energy loss in dense matter (M. Djordjevic *et al.*, Z. Lin *et al.*, D. Kharzeev and Yu. Dokshitzer)**
- **Transverse momentum broadening due to hadronization from quark-gluon plasma (B. Svetitsky) or cold nuclear matter**
- **Collective flow of charm quarks (Z. Lin and D. Molnar, R. Rapp *et al.*)**

In addition, if multiple $c\bar{c}$ pairs are produced in a given event, can enhance J/ψ (hidden charm) production (R. Thews *et al.*)

pp and d+Au collisions serve as an important baseline for understanding medium effects on charm production, need good theoretical background and up-to-date open charm data

Charm and Bottom Hadrons

Imperative to measure more than one type of heavy flavor hadron to obtain total $Q\overline{Q}$ cross section

C	**Mass (GeV)**	$c\tau$ **(μm)**	$B(C \to lX)$ **(%)**	$B(C \to$ Hadrons**)** **(%)**
$D^+(c\bar{d})/D^-(\bar{c}d)$	**1.869**	**315**	**17.2**	$K^\mp\pi^\pm\pi^\pm$ **(9.1)**
$D^0(c\bar{u})/\overline{D^0}(\bar{c}u)$	**1.864**	**123.4**	**6.87**	$K^\mp\pi^\pm$ **(3.8)**
$D^{*+}(c\bar{d})/D^{*-}(\bar{c}d)$	**2.010**			$D^0\pi^\pm$ **(67.7)**, $D^\pm\pi^0$ **(30.7)**
$D^{*0}(c\bar{u})/\overline{D^{*0}}(\bar{c}u)$	**2.007**			$D^0\pi^0$ **(61.9)**
$D_s^+(c\bar{s})/D_s^-(\bar{c}s)$	**1.969**	**147**	**8**	$K^+K^-\pi^\pm$ **(4.4)**, $\pi^+\pi^-\pi^\pm$ **(1.01)**
$\Lambda_c^+(udc)$	**2.285**	**59.9**	**4.5**	ΛX **(35)**, $pK^-\pi^+$ **(2.8)**
$B^0(d\bar{b})/\overline{B^0}(\bar{d}b)$	**5.2794**	**460**	**10.5**	$D^\mp\pi^\pm$ **(0.276)**, $J/\psi K^\pm\pi^\mp$ **(0.0325)**
$B^+(u\bar{b})/B^-(\bar{u}b)$	**5.2790**	**501**	**10.2**	$\overline{D}^0\pi^\mp\pi^\pm\pi^\pm$ **(1.1)**, $J/\psi K^\pm$ **(0.1)**
$B_s^0(s\bar{b})/\overline{B_s^0}(\bar{s}b)$	**5.3696**	**438**		$D_s^\mp\pi^\pm$ **(<13)**
$B_c^+(c\bar{b})/B_c^-(\bar{c}b)$	**6.4**			$J/\psi\pi^\pm$ **(0.0082)**
$\Lambda_b^0(udb)$	**5.624**	**368**		$J/\psi\Lambda$ **(0.047)**, $\Lambda_c^+\pi^-$ **(seen)**

Table 1: Some ground state charm and bottom hadrons with their mass, decay length (when given) and branching ratios to leptons (when applicable) and some prominent decays to hadrons, preferably to only charged hadrons although such decays are not always available.

Calculating Heavy Flavors in Perturbative QCD

'Hard' processes have a large scale in the calculation that makes perturbative QCD applicable: high momentum transfer, μ^2, high mass, m, high transverse momentum, p_T, since $m \neq 0$, heavy quark production is a 'hard' process

Factorization assumed between the perturbative hard part and the universal, non-perturbative parton distribution functions

Hadronic cross section in an AB collision where $AB = pp, pA$ or nucleus-nucleus is

$$\sigma_{AB}(S, m^2) = \sum_{i,j=q,\overline{q},g} \int_{4m_Q^2/s}^1 \frac{d\tau}{\tau} \int dx_1\, dx_2\, \delta(x_1 x_2 - \tau) f_i^A(x_1, \mu_F^2)\, f_j^B(x_2, \mu_F^2)\, \widehat{\sigma}_{ij}(s, m^2, \mu_F^2, \mu_R^2)$$

f_i^A are the nonperturbative parton distributions, determined from fits to data, x_1 and x_2 are the fractional momentum of hadrons A and B carried by partons i and j, $\tau = s/S$

$\widehat{\sigma}_{ij}(s, m^2, \mu_F^2, \mu_R^2)$ is hard partonic cross section calculable in QCD in powers of α_s^{2+n}: leading order (LO), $n = 0$; next-to-leading order (NLO), $n = 1$ ...

Results depend strongly on quark mass, m, factorization scale, μ_F, in the parton densities and renormalization scale, μ_R, in α_s

Calculating the Total Cross Sections

Partonic total cross section only depends on quark mass m, not kinematic quantities

Only available to NLO, not higher order

To NLO

$$\begin{aligned}\widehat{\sigma}_{ij}(s, m, \mu_F^2, \mu_R^2) &= \frac{\alpha_s^2(\mu_R^2)}{m^2}\left\{ f_{ij}^{(0,0)}(\rho) \right. \\ &+ \left. 4\pi\alpha_s(\mu_R^2)\left[f_{ij}^{(1,0)}(\rho) + f_{ij}^{(1,1)}(\rho)\ln(\mu_F^2/m^2)\right] + \mathcal{O}(\alpha_s^2)\right\}\end{aligned}$$

$\rho = 4m^2/s$, s is partonic center of mass energy squared

μ_F is factorization scale, separates hard part from nonperturbative part

μ_R is renormalization scale, scale at which strong coupling constant α_s is evaluated

$\mu_F = \mu_R$ in evaluations of parton densities

$f_{ij}^{(a,b)}$ are dimensionless, μ-independent scaling functions, $a = 0$, $b = 0$ and $ij = q\overline{q}$, gg for LO, $a = 1$, $b = 0, 1$ and $ij = q\overline{q}$, gg and qg, $\overline{q}g$ for NLO

$f_{ij}^{(0,0)}$ are always positive, $f_{ij}^{(1,b)}$ can be negative also

Note that if $\mu_F^2 = m^2$, $f_{ij}^{(1,1)}$ does not contribute

Scaling Functions to NLO

Near threshold, $\sqrt{S}/2m \to 1$, Born contribution is large but dies away for $\sqrt{S}/2m \to \infty$

At large $\sqrt{S}/2m$, gg channel is dominant, then qg

High energy behavior of the cross sections due to phase space and low x behavior of parton densities

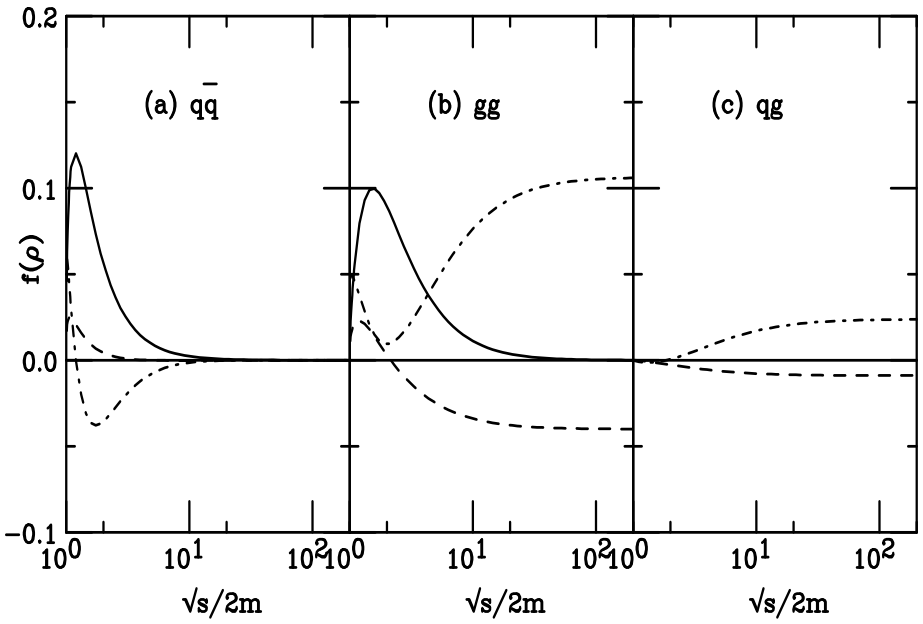

Figure 1: Scaling functions needed to calculate the total partonic $Q\overline{Q}$ cross section. The solid curves are the Born results, $f_{ij}^{(0,0)}$, the dashed and dot-dashed curves are NLO contributions, $f_{ij}^{(1,1)}$ and $f_{ij}^{(1,0)}$ respectively.

Choosing Parameters

Two important parameters: the quark mass m and the scale μ – at high energies, far from threshold, the low x, low μ behavior of the parton densities determines the charm result, bottom less sensitive to parameter choice

The scale is usually chosen so that $\mu_F = \mu_R$, as in parton density fits, no strict reason for doing so for heavy flavors

Two ways to make predictions:

Fit to Data (RV, Hard Probes Collaboration): fix m and $\mu \equiv \mu_F = \mu_R \geq m$ to data at lower energies and extrapolate to unknown regions – favors lower m

Uncertainty Band (Cacciari, Nason and RV): band determined from mass range, $1.3 < m < 1.7$ GeV (charm) and $4.5 < m < 5$ GeV (bottom) with $\mu_F = \mu_R = m$, and range of scales relative to central mass value, $m = 1.5$ GeV (charm) and 4.75 GeV (bottom): $(\mu_F/m, \mu_R/m) = (1,1)$, (2,2), (0.5,0.5), (0.5,1), (1,0.5), (1,2), (2,1) (Ratio is relative to m_T for distributions)

Need to be careful with $\mu_F \leq m$ and the CTEQ6M parton densities since $\mu_{\rm min} = 1.3$ GeV, gives big K factors for low scales – problem occurs at low p_T

Densities like GRV98 have lower $\mu_{\rm min}$ so low x, low μ behavior less problematic
Value of two-loop α_s is big for low scales, for $m = 1.5$ GeV:
$\alpha_s(m/2 = 0.75\ {\rm GeV}) = 0.648$, $\alpha_s(m = 1.5\ {\rm GeV}) = 0.348$ **and** $\alpha_s(2m = 3\ {\rm GeV}) = 0.246$

CTEQ6M Densities at $\mu = m/2$, m and $2m$

CTEQ6M densities extrapolate to $\mu < \mu_{\min} = 1.3$ GeV

When backwards extrapolation leads to $xg(x,\mu) < 0$, then $xg(x,\mu) \equiv 0$

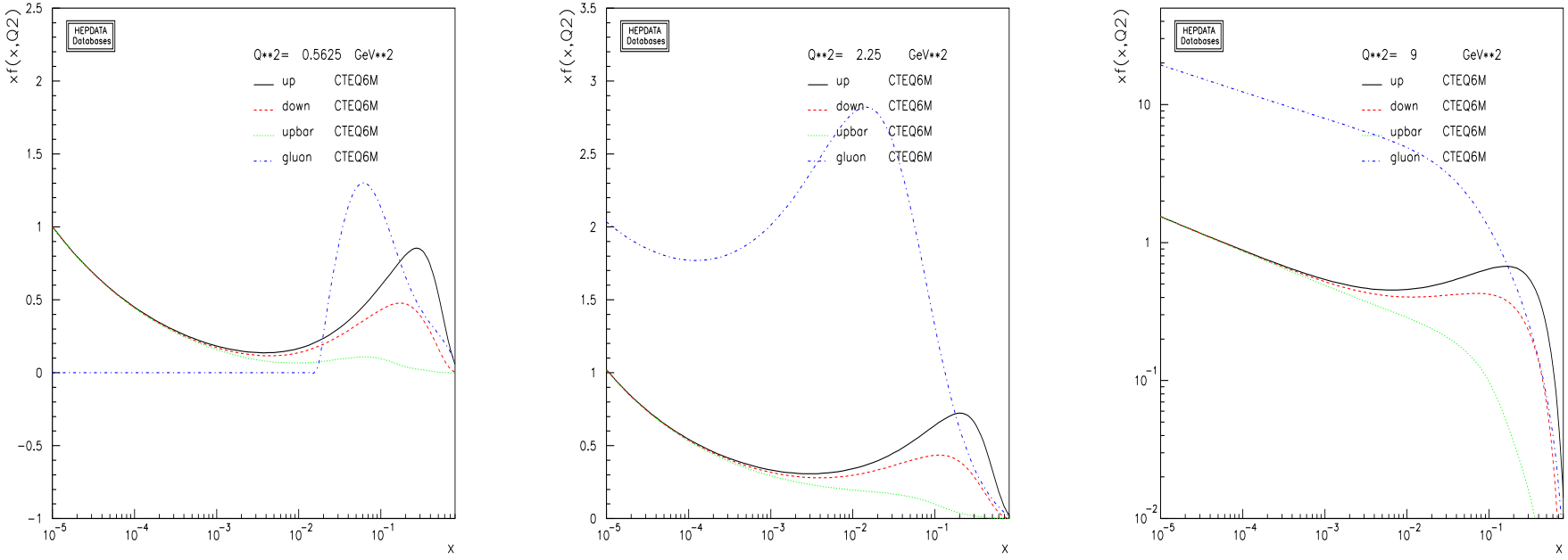

Figure 2: The CTEQ6M parton densities as a function of x for $\mu = m/2$ (left), $\mu = m$ (middle) and $\mu = 2m$ (right) for $m = 1.5$ GeV.

Charm Total Cross Section Uncertainty Band

The $\mu_F \leq m$ results flatten at $\sqrt{S} > 100$ GeV: low x, low μ behavior of CTEQ6M

$(\mu_F/m, \mu_R/m) = (1, 0.5)$ and (0.5,0.5) have large total cross sections at RHIC since α_s big

Evolution faster at small x and high μ [(2,2), (2,1)]

'Fit' with $m = 1.2$ GeV, $(\mu_F/m, \mu_R/m) = (2, 2)$ shown in black

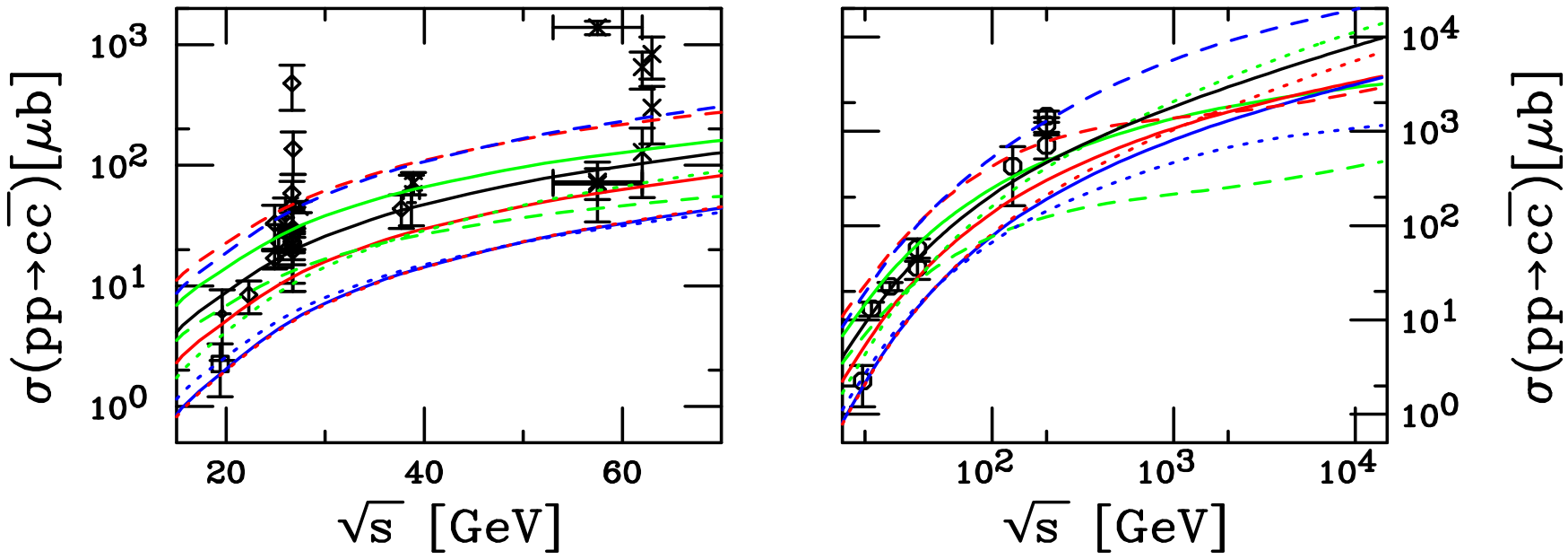

Figure 3: Total $c\bar{c}$ cross sections calculated using CTEQ6M. The solid red curve is the central value $(\mu_F/m, \mu_R/m) = (1, 1)$ with $m = 1.5$ GeV. The green and blue solid curves are $m = 1.3$ and 1.7 GeV with (1,1) respectively. The red, blue and green dashed curves correspond to (0.5,0.5), (0.5,1) and (1,0.5) respectively while the red, blue and green dotted curves are for (2,2), (2,1) and (1,2) respectively, all for $m = 1.5$ GeV. The black curve is $m = 1.2$ GeV with (2,2).

K Factors of Total Charm Cross Section

Calculations with $\mu_F \leq m$ have large K factors

Bigger scales and $\mu_F = \mu_R$ have smallest K factors

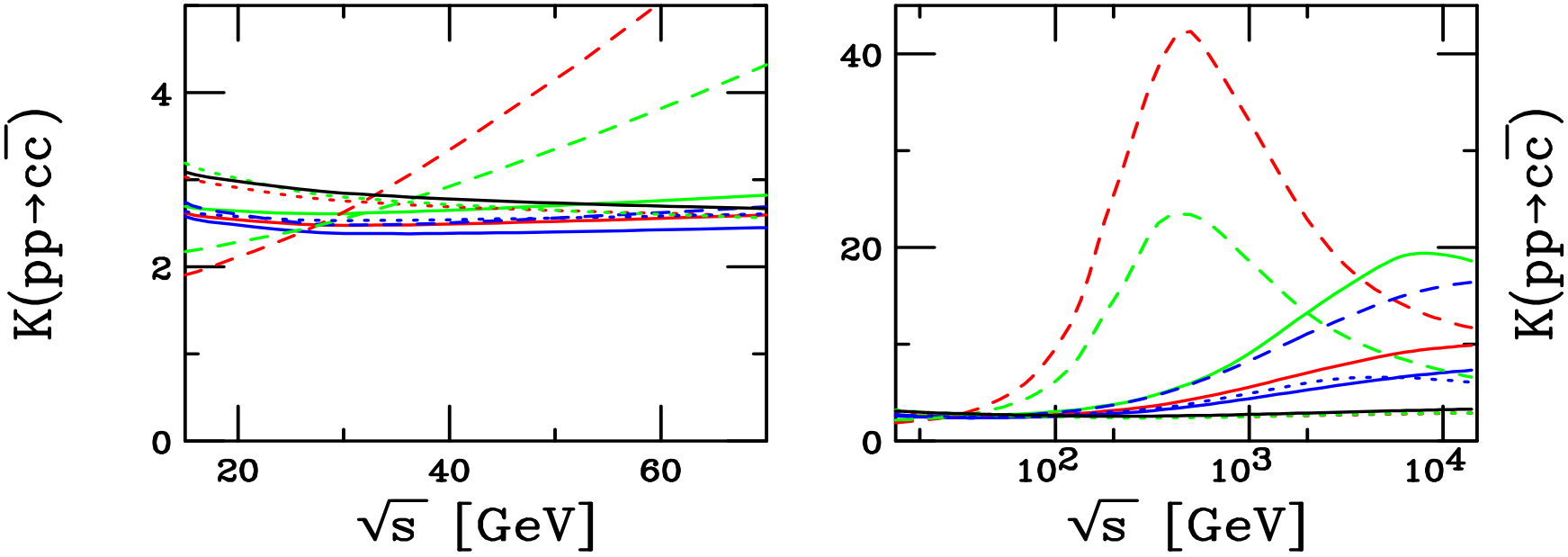

Figure 4: Theoretical K factors calculated using CTEQ6M. The solid red curve is the central value $(\mu_F/m, \mu_R/m) = (1, 1)$ with $m = 1.5$ GeV. The green and blue solid curves are $m = 1.3$ and 1.7 GeV with (1,1) respectively. The red, blue and green dashed curves correspond to (0.5,0.5), (0.5,1) and (1,0.5) respectively while the red, blue and green dotted curves are for (2,2), (2,1) and (1,2) respectively, all for $m = 1.5$ GeV. The black curve is $m = 1.2$ GeV with (2,2).

Bottom Total Cross Section Uncertainty Band

Larger scales make band narrower over all energies

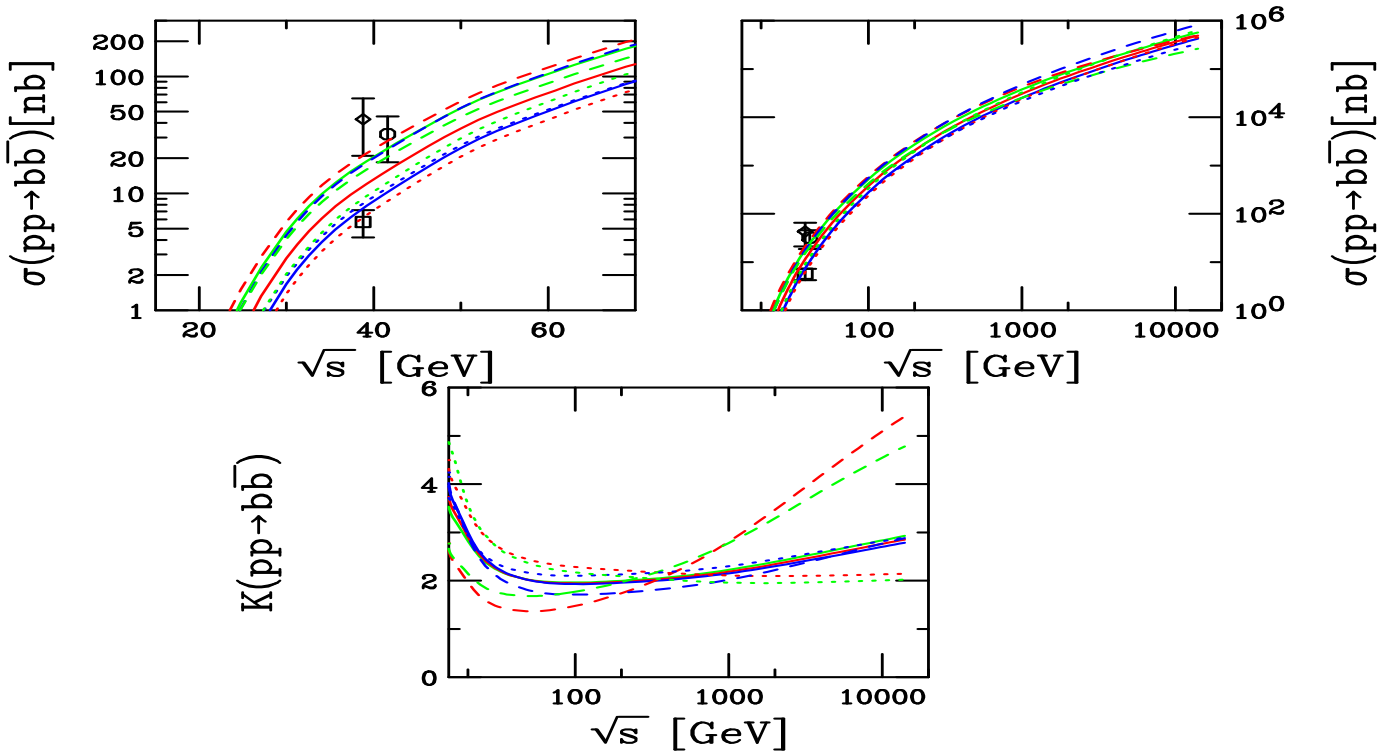

Figure 5: Total $b\bar{b}$ cross sections calculated using CTEQ6M. The solid red curve is the central value $(\mu_F/m, \mu_R/m) = (1, 1)$ with $m = 4.75$ GeV. The green and blue solid curves are $m = 4.5$ and 5 GeV with (1,1) respectively. The red, blue and green dashed curves correspond to (0.5,0.5), (1,0.5) and (0.5,1) respectively while the red, blue and green dotted curves are for (2,2), (1,2) and (2,1) respectively, all for $m = 4.75$ GeV.

From Total Cross Sections to Distributions

Distributions as a function of kinematic variables can provide more information than the total cross section

Quark mass only relevant scale for total cross sections, not for distributions

When considering kinematic observables, the momentum scale is also relevant so that, instead of $\mu^2 \propto m^2$, one usually uses $\mu^2 \propto m_T^2$ – slightly affects the p_T-integrated total cross section

Fragmentation universal, like parton densities, so the parameterizations of e^+e^- data should work in hadroproduction

New determinations of the charm to D fragmentation in Mellin space result in a softer, more accurate spectra than the old Peterson function

The b quark fragmentation is very hard, b and B p_T distributions similar

FONLL Calculation (Cacciari and Nason)

Designed to cure large logs of p_T/m for $p_T \gg m$ in fixed order calculation (FO) where mass is no longer only relevant scale

Includes resummed terms (RS) of order $\alpha_s^2(\alpha_s \log(p_T/m))^k$ (leading log – LL) and $\alpha_s^3(\alpha_s \log(p_T/m))^k$ (NLL) while subtracting off fixed order terms retaining only the logarithmic mass dependence (the "massless" limit of fixed order (FOM0)), both calculated in the same renormalization scheme

Scheme change needed in the FO calculation since it treats the heavy flavor as heavy while the RS approach includes the heavy flavor as an active light degree of freedom

Schematically:

$$\mathrm{FONLL} = \mathrm{FO} + (\mathrm{RS} - \mathrm{FOM0})\ G(m, p_T)$$

$G(m, p_T)$ is arbitrary but $G(m, p_T) \to 1$ as $m/p_T \to 0$ up to terms suppressed by powers of m/p_T

Total cross section similar to but slightly higher than NLO

Problems at high energies away from midrapidity due to small x, high z behavior of fragmentation functions in RS result, therefore we don't calculate results for $|y| > 2$, worse for LHC predictions

Comparison of FONLL and NLO p_T Distributions

FONLL result for bare charm is slightly higher over most of the p_T range – fixed order result gets higher at large p_T due to large $\log(p_T/m)$ terms

New D^0 fragmentation functions (dashed) harder than Peterson function (dot-dot-dot-dashed)

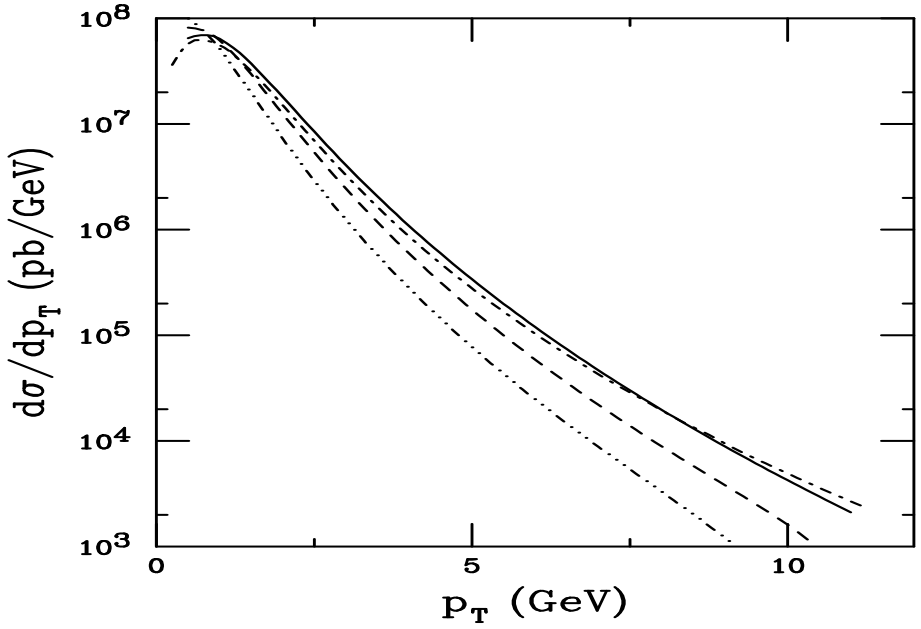

Figure 6: The p_T distributions calculated using FONLL are compared to NLO. The dot-dashed curve is the NLO charm quark p_T distribution. The solid, dashed and dot-dot-dot-dashed curves are FONLL results for the charm quark and D^0 meson with the updated fragmentation function and the Peterson function, respectively. All the calculations are done with the CTEQ6M parton densities, $m = 1.2$ GeV and $\mu = 2m_T$ in the region $|y| \leq 0.75$.

Uncertainty Bands for p_T Distributions

Due to range of parameters chosen for uncertainty band, the maximum and minimum result as a function of p_T may not come from a single set of parameters

Thus the upper and lower curves in the band do not represent a single set of μ_R, μ_F and m values but are the upper and lower limits of mass and scale uncertainties added in quadrature:

$$\frac{d\sigma_{\rm max}}{dp_T} = \frac{d\sigma_{\rm cent}}{dp_T} + \sqrt{\left(\frac{d\sigma_{\mu,\rm max}}{dp_T} - \frac{d\sigma_{\rm cent}}{dp_T}\right)^2 + \left(\frac{d\sigma_{m,\rm max}}{dp_T} - \frac{d\sigma_{\rm cent}}{dp_T}\right)^2}$$

$$\frac{d\sigma_{\rm min}}{dp_T} = \frac{d\sigma_{\rm cent}}{dp_T} - \sqrt{\left(\frac{d\sigma_{\mu,\rm min}}{dp_T} - \frac{d\sigma_{\rm cent}}{dp_T}\right)^2 + \left(\frac{d\sigma_{m,\rm min}}{dp_T} - \frac{d\sigma_{\rm cent}}{dp_T}\right)^2}$$

The central values are $m = 1.5$ GeV (charm) and 4.75 GeV (bottom), $\mu_F = \mu_R = m_T$

We follow the same procedure for both the NLO and FONLL calculations and compare them in the central ($|y| \leq 0.75$) and forward ($1.2 < y < 2.2 - 1.2 < y < 2$ for FONLL) regions

Previous (HPC) charm results with $m = 1.2$ GeV, $\mu_F = \mu_R = 2m_T$ fall within the uncertainty band

Bare heavy quark and heavy flavor meson p_T distributions shown for pp collisions at $\sqrt{S} = 200$ GeV and 5.5 TeV

Comparison to STAR d+Au D Data

Agreement of upper limit of uncertainty band with low p_T STAR data rather reasonable

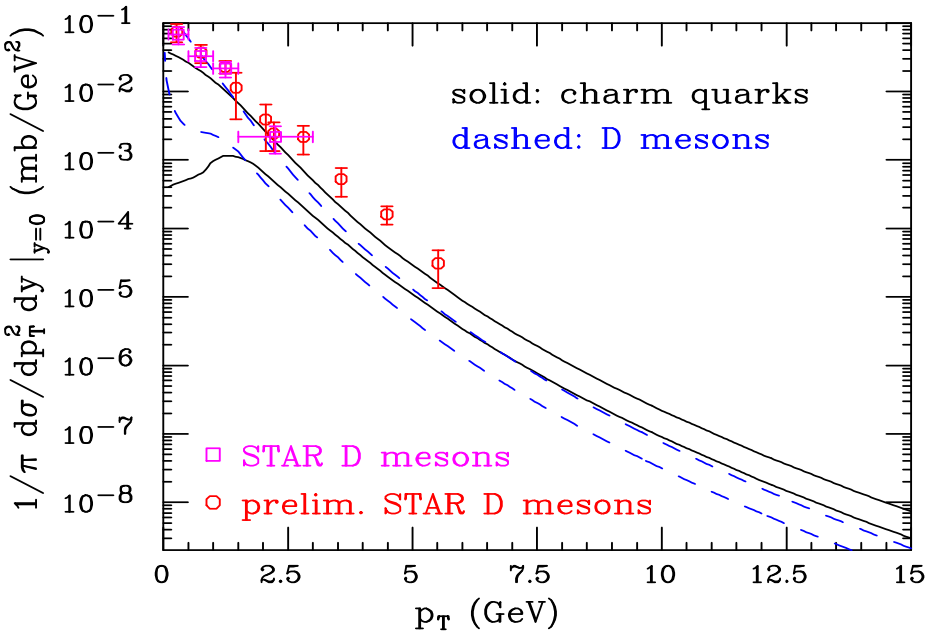

Figure 7: The FONLL theoretical uncertainty bands for the charm quark and D meson p_T distributions in pp collisions at $\sqrt{S} = 200$ GeV, using BR($c \to D$) = 1. Both final and preliminary STAR d+Au data (scaled to pp using $N_{\rm bin} = 7.5$) at $\sqrt{S_{NN}} = 200$ GeV are also shown.

Uncertainty Bands for c and D at 5.5 TeV

c and D distributions are harder at 5.5 TeV

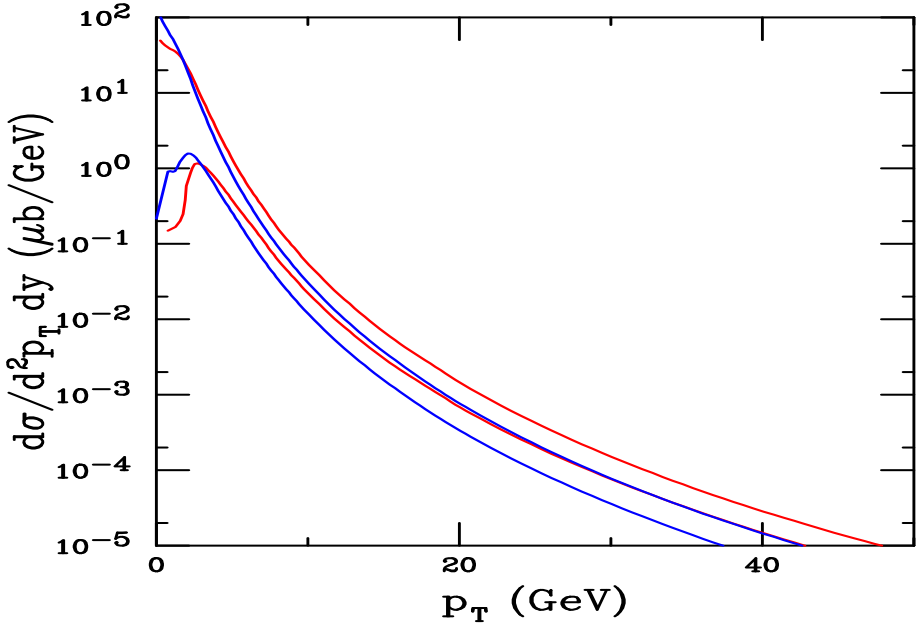

Figure 8: The charm quark theoretical uncertainty band as a function of p_T at NLO (red curves) in $\sqrt{S} = 5.5$ TeV pp collisions. Also shown is the D meson uncertainty band (blue curves), all using the CTEQ6M parton densities for $|y| \leq 1$.

Uncertainty Bands for b and B at 200 GeV

Bands narrower for bottom than for charm and impossible to separate b from B over the p_T range shown (B is a generic B meson)

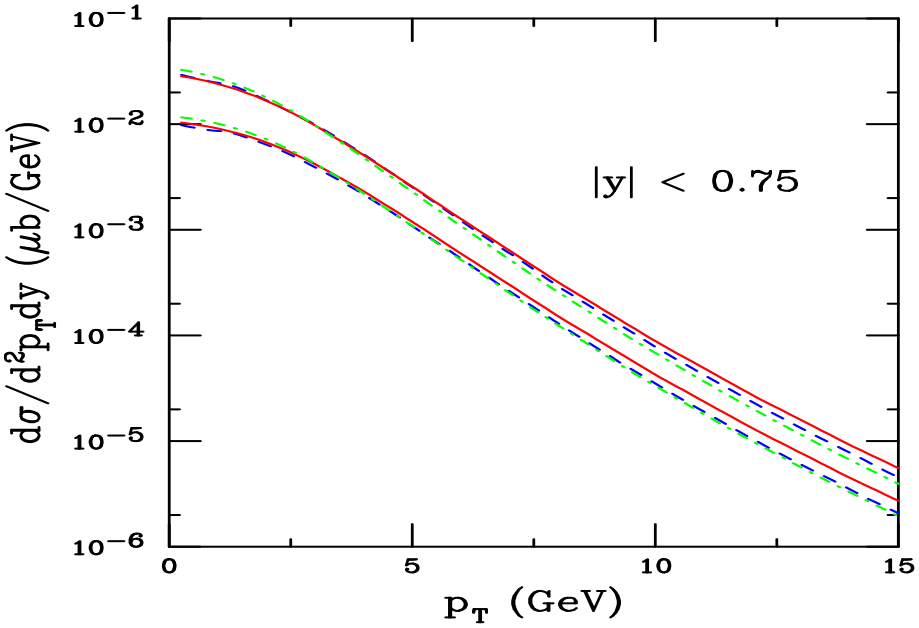

Figure 9: The bottom quark theoretical uncertainty band as a function of p_T for FONLL (red solid curves) and NLO (blue dashed curves) in $\sqrt{S} = 200$ GeV pp collisions. Also shown is the B meson uncertainty band (green dot-dashed curves), all using the CTEQ6M parton densities for $|y| \leq 0.75$.

Uncertainty Bands for b and B at 5.5 TeV

Much stronger energy dependence and more hardening for bottom than for charm with increasing energy

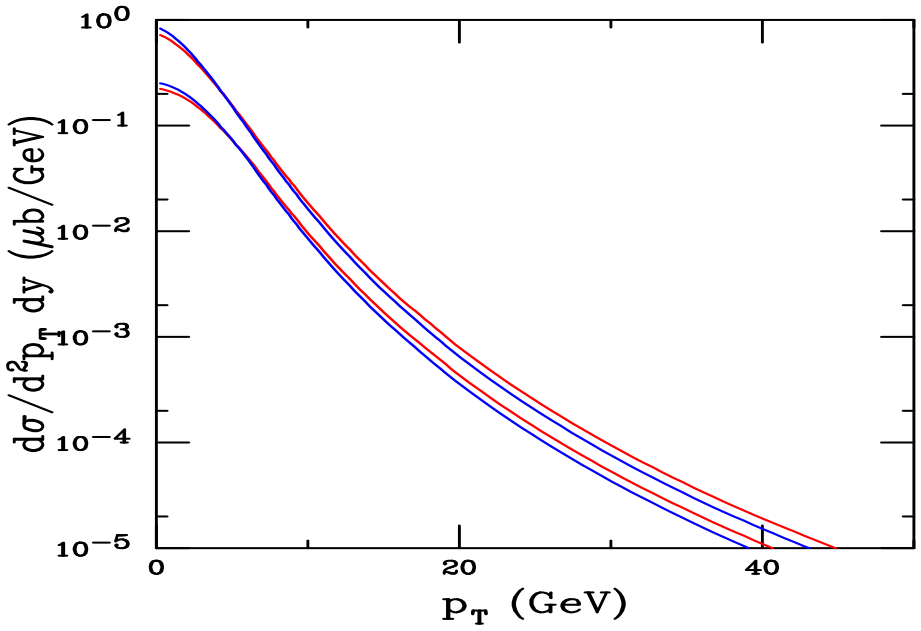

Figure 10: The bottom quark theoretical uncertainty band as a function of p_T at NLO (red curves) in $\sqrt{S} = 5.5$ TeV pp collisions. Also shown is the B meson uncertainty band (blue curves), all using the CTEQ6M parton densities for $|y| \leq 1$.

Obtaining the Electron Spectra From Heavy Flavor Decays

D and B decays to leptons depends on measured decay spectra and branching ratios

- **$D \to e$ Use preliminary CLEO data on inclusive electrons from semi-leptonic D decays, assume it to be indentical for all charm hadrons**
- **$B \to e$ Primary B decays to electrons measured by Babar and CLEO, fit data and assume fit to work for all bottom hadrons**
- **$B \to D \to e$ Obtain electron spectrum from convolution of $D \to e$ spectrum with parton model calculation of $b \to c$ decay**

Branching ratios are admixtures of charm and bottom hadrons

$$\begin{aligned} B(D \to e) &= 10.3 \pm 1.2\,\% \\ B(B \to e) &= 10.86 \pm 0.35\,\% \\ B(B \to D \to e) &= 9.6 \pm 0.6\,\% \end{aligned}$$

Uncertainty Bands for Electrons from Heavy Flavor Decays at 200 GeV

Electrons from B decays begin to dominate at $p_T \sim 5$ GeV

Electron spectra very sensitive to rapidity range – to get $|y| \leq 0.75$ electrons, need $|y| \leq 2$ charm and bottom range

Forward electron spectra thus not possible to obtain using FONLL code due to problems at large y

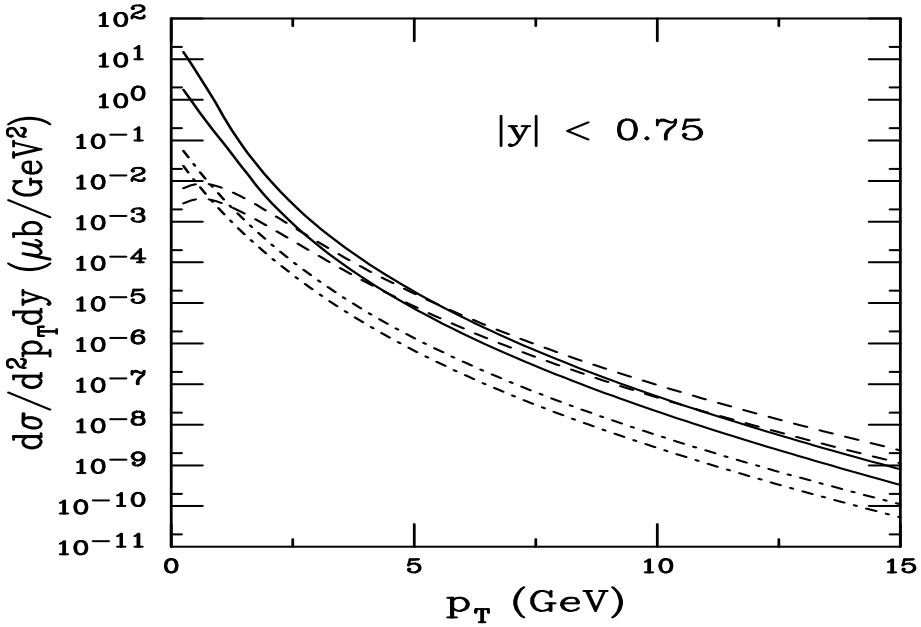

Figure 11: The theoretical FONLL bands for $D \to eX$ (solid), $B \to eX$ (dashed) and $B \to DX \to eX'$ (dot-dashed) as a function of p_T in $\sqrt{S} = 200$ GeV pp collisions for $|y| < 0.75$.

Location of b/c Crossover Sensitive to Details of Fragmentation Scheme, Scales, Quark Mass

The $b \to e$ decays dominate at lower p_T when Peterson function ($\epsilon_c = 0.06, \epsilon_b = 0.006$) is used since it steepens charm p_T spectra more than bottom

Ratios here shown with scales correlated, uncorrelated scales would broaden crossover region

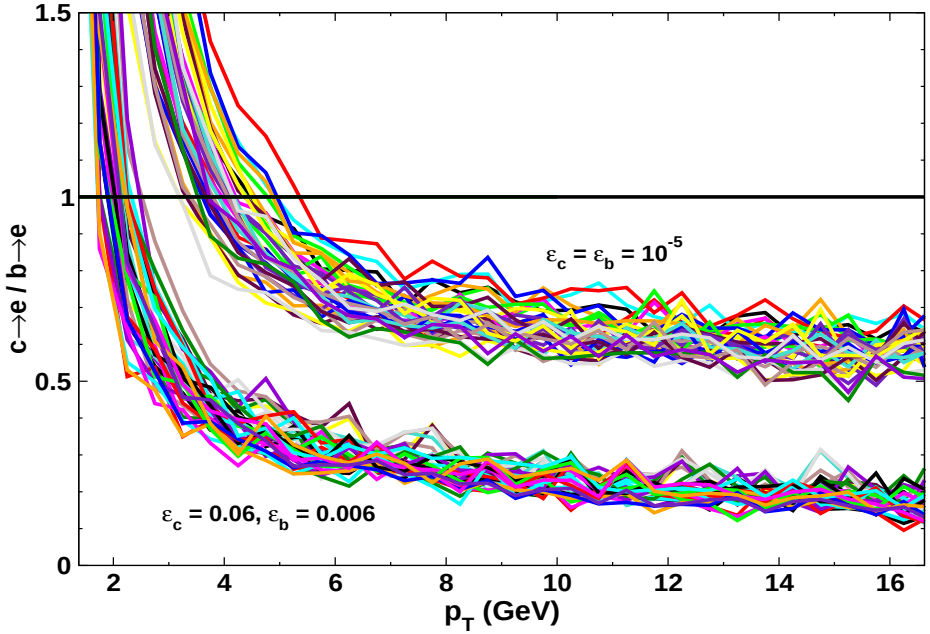

Figure 12: The ratio of charm to bottom decays to electrons obtained by varying the quark mass and scale factors. The effect of changing the Peterson function parameters from $\epsilon_c = 0.06$, $\epsilon_b = 0.006$ (lower band) to $\epsilon_c = \epsilon_b = 10^{-5}$ (upper band) is also illustrated. (From M. Djordjevic *et al.*.)

Comparison to Electron Data at 200 GeV

Includes PHENIX preliminary data from *pp* and STAR published and preliminary data

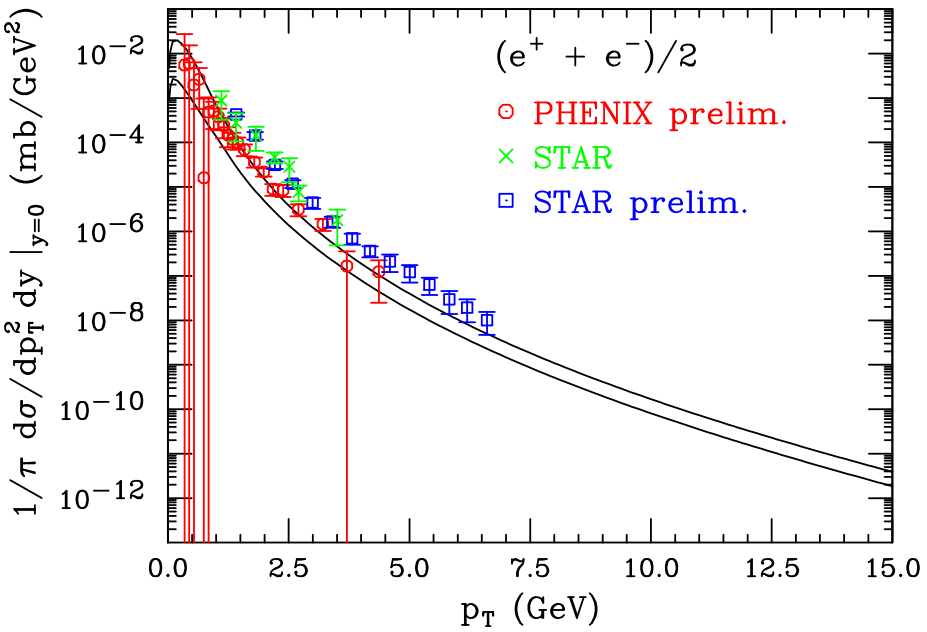

Figure 13: Prediction of the theoretical uncertainty band of the total electron spectrum from charm and bottom (Cacciari, Nason and RV). Preliminary data from PHENIX and STAR are also shown.

Uncertainty Bands for Electrons from Heavy Flavor Decays at 5.5 TeV

Crossover between B and D dominance harder to distinguish at LHC energy since $\sqrt{S_{NN}} \gg m_Q$ for charm *and* bottom

Electron spectra much harder with increased energy

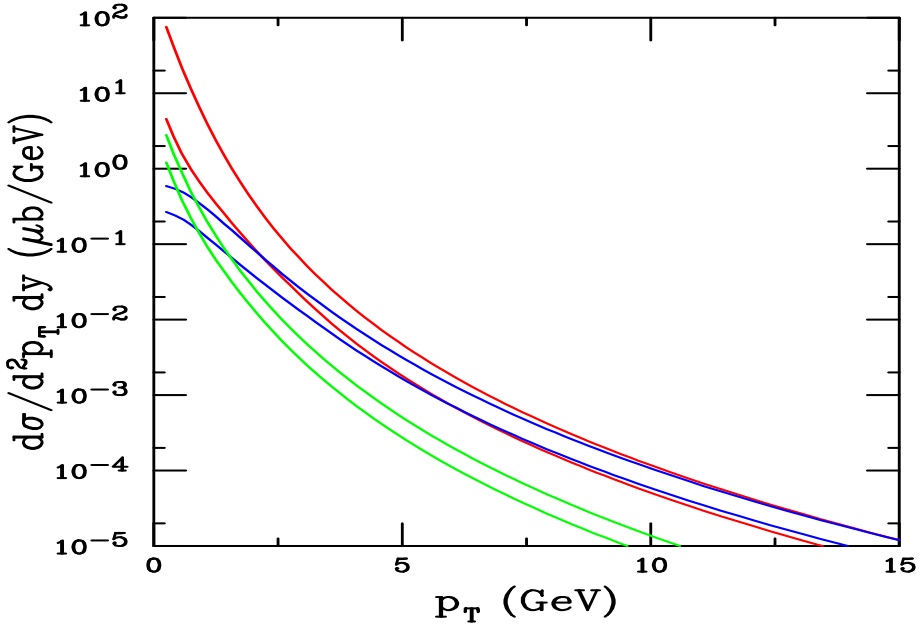

Figure 14: The theoretical bands for $D \to eX$ (red curves), $B \to eX$ (blue curves) and $B \to DX \to eX'$ (green curves) as a function of p_T in $\sqrt{S} = 5.5$ TeV pp collisions for $|y| < 1$.

Summary .

- Theoretical uncertainty bands at low p_T show effects of low x and low μ behavior of parton densities .
- More modern fragmentation functions for D and B mesons indicate that the meson distribution is more similar to the quark distribution to higher p_T than previously assumed from older e^+e^- fits
- Contributions of D and B decays to leptons more difficult to disentangle at LHC and would require precision measurements of their decays to hadrons to better distinguish .
- Variety of decay channels needed to sort out results

HAPPY BIRTHDAY, HELMUT – MANY, MANY MORE!!!!